

Electronic Supplementary Information, ESI

**Structural and Tribological Characterization of Fluorinated Graphene with
Various Fluorine Contents Prepared by Liquid-Phase Exfoliation**

Kaiming Hou^{a,b}, Peiwei Gong^{a,b}, Jinqing Wang^{a,*}, Zhigang Yang^a,

Zhaofeng Wang^a, and Shengrong Yang^{a,*}

^a State Key Laboratory of Solid Lubrication, Lanzhou Institute of Chemical Physics,

Chinese Academy of Sciences, Lanzhou, 730000, P. R. China.

^b University of Chinese Academy of Sciences, Beijing, 100080, P. R. China.

* Corresponding author.

Tel./Fax: +86 931 4968076. E-mail address: jqwang@licp.cas.cn (J. Q. Wang)

1. HRTEM micrographs of the obtained FG

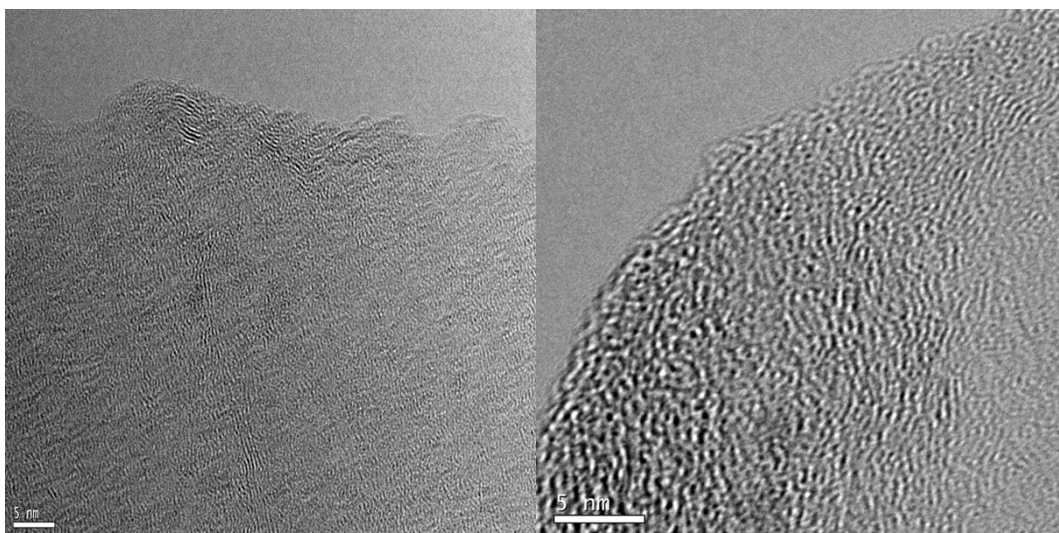


Fig. S1 gives the HRTEM images of few-layer FG sheet exfoliated from FGi. It can be observed that the prepared FG sheet has no hexagonal arrangement and presents a disordered characteristic.

2. XRD patterns of the pristine FGi and FG samples

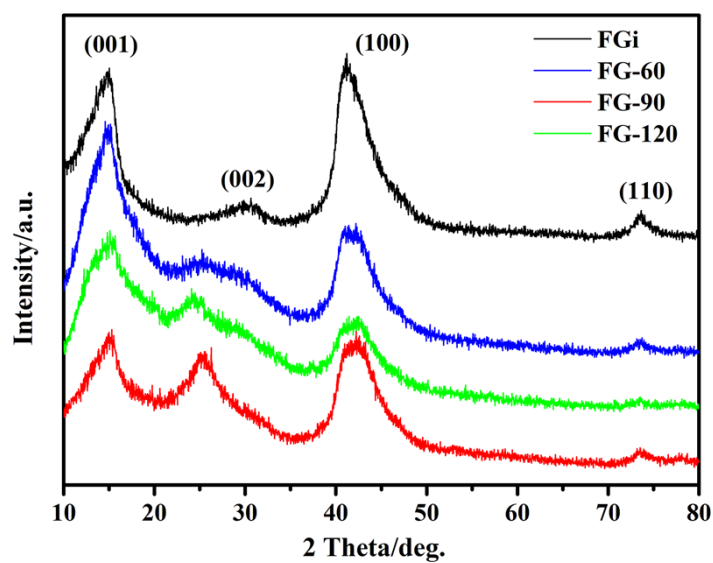


Fig. S2 gives the XRD patterns of the pristine FGi and FG samples obtained at different reaction temperatures. The peak at 14.8° for all samples is a (001) reflection with a d-spacing of 0.560 nm in a hexagonal system. The intensity of the peak increases with the increase of fluorine contents. The appearance of a broad peak corresponding to the (002) diffraction of graphite structures suggests the samples are disordered and randomly stacked along the stacking direction. Compared with FGi, the (002) peak of FG samples shifts to lower 2θ degree accompanied with an increase of peak intensity. This suggests the FG samples get wider interlayer spacing and effective intercalation and exfoliation are realized, meanwhile, with the increase of reduction degree (restoration of sp^2 bonding in the graphitized carbon sheet). The peak at around 42° corresponding to (100) reflection is associated with the C-C in-plane length in the reticular system.

3. FT-IR spectrum and XPS survey spectrum of FGi

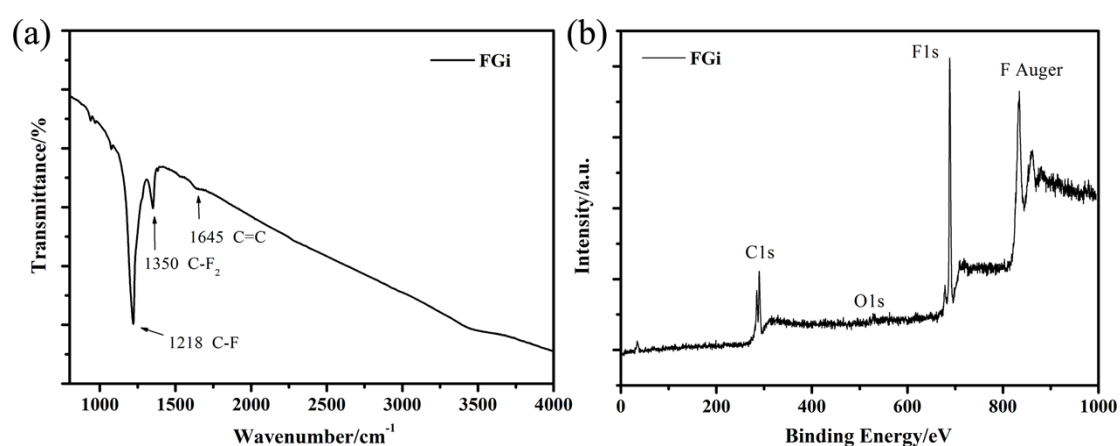


Fig. S3 provides FT-IR spectrum (a) and XPS survey spectrum (b) of FGi. Due to fact that the physicochemical property of FGi is strongly dependent on its synthetic

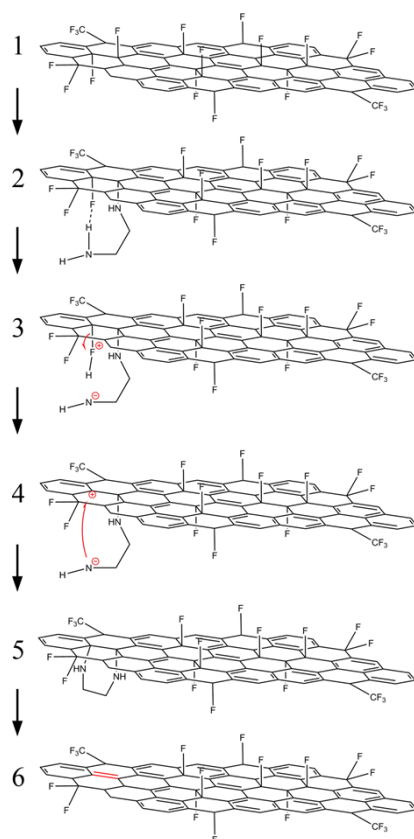
conditions, detailed composition information of the starting commercial FGi needs to be known. As shown in the FT-IR spectrum, the absorption peak position of FGi is similar with that of FG. The difference is that the peaks corresponding to C-F and C-F₂ have a higher intensity for FGi. The XPS survey spectrum indicates that only C, F and trace amounts of O are detected. The fluorine content is 51.29-51.47 atom %, suggesting the FGi has no impurities and possesses a high fluorine level.

4. Proposed mechanism for defluorination reduction caused by EDA.

Previous studies pointed out that hydrazine has apparent reductability to fluorinated graphene (FG) and fluorinated single-wall carbon nanotubes.^{1,2} They thought the reduction proceeds likely as the reaction of $4CF_n + nN_2H_4 \rightarrow 4C + 4nHF + 2nN_2$. Unlike hydrazine which is a kind of highly active reducing agent, ethylenediamine (EDA) has mild reducing property and its structure would remain stable in the reaction rather than decompose. So this explanation on hydrazine is not suitable for explanation of defluorination reduction.

Although it is found that in functionalization reactions of fluorinated carbon materials the phenomenon of elimination and substitution of fluorine carried out synchronously is very common,³⁻⁸ it is still hard to propose a unambiguous mechanism to explain the experiment results, because previous works can't provide much more insight into the reason for partial reduction in the carbon lattice. Nevertheless, according to the report on chemical reduction between graphene oxide (GO) and EDA,⁹ a possible explanation considering that the hydroxyls in GO and fluorines in FG are

isoelectronic and have similar polarity can be established for a better understanding of the reaction mechanism.



Scheme S1. Cyclization-removal defluorination mechanism of FG reduction performed by EDA

Firstly, fluorine can be substituted accompanied with the formation of C-N bond through nucleophilic substitution. Then primary amine group at the free terminal further reacts with its adjacent fluorine, which lead to elimination of the fluorine and subsequently conducts cyclization. After that, the cycle form is not stable due to the large tension and a removal reaction would happen. Hence, double bond can be introduced into the hexagonal network. The detailed process is shown in Scheme S1.

REFERENCES

- 1 J. T. Robinson, J. S. Burgess, C. E. Junkermeier, S. C. Badescu, T. L. Reinecke, F. K. Perkins, M. K. Zalalutdniov, J. W. Baldwin, J. C. Culbertson, P. E. Sheehan and E. S. Snow, *Nano Lett.*, 2010, **10**, 3001-3005.
- 2 E. T. Mickelson, C. B. Huffman, A. G. Rinzler, R. E. Smalley, R. H. Hauge and J. L. Margrave, *Chem. Phys. Lett.*, 1998, **296**, 188-194.
- 3 L. Valentini, M. Cardinali, S. B. Bon, D. Bagnis, R. Verdejo, M. A. Lopez-Manchado and J. M. Kenny, *J. Mater. Chem.*, 2010, **20**, 995-1000.
- 4 K. A. Worsley, P. Ramesh, S. K. Mandal, S. Niyogi, M. E. Itkis and R. C. Haddon, *Chem. Phys. Lett.*, 2007, **445**, 51-56.
- 5 R. Stine, J. W. Ciszek, D. E. Barlow, W. Lee, J. T. Robinson and P. E. Sheehan, *Langmuir*, 2012, **28**, 7957-7961.
- 6 K. Bushimata, S. Ogino, K. Hirano, T. Yabune, K. Sato, T. Itoh, K. Motomiya, K. Yokoyama, D. Mabuchi, H. Nishizaka, G. Yamamoto, T. Hashida, K. Tohji and Y. Sato, *J. Phys. Chem. C*, 2014, **118**, 14948-14956.
- 7 J. L. Stevens, A. Y. Huang, H. Peng, I. W. Chiang, V. N. Khabashesku and J. L. Margrave, *Nano Lett.*, 2003, **3**, 331-336.
- 8 L. Zhang, V. U. Kiny, H. Peng, J. Zhu, R. F. M. Lobo, J. L. Margrave and V. N. Khabashesku, *Chem. Mater.*, 2004, **16**, 2055-2061.
- 9 J. Che, L. Shen and Y. Xiao, *J. Mater. Chem.*, 2010, **20**, 1722-1727.

5. UV-Vis absorption spectra of the FG samples

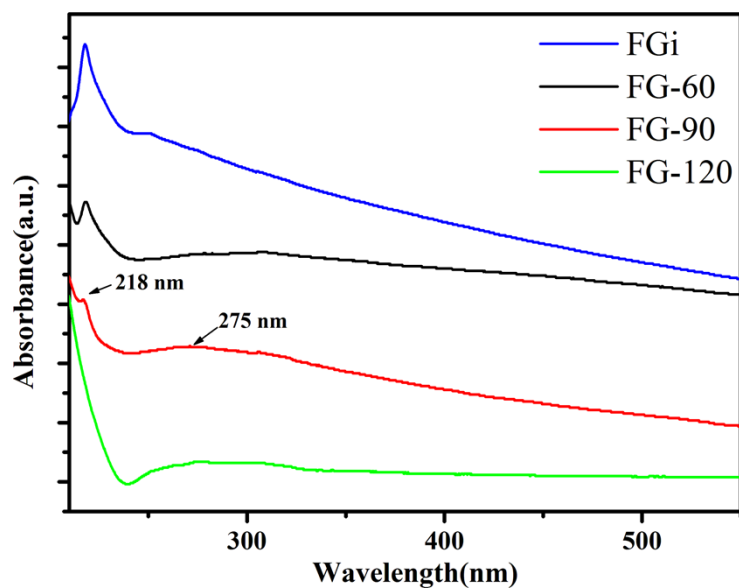


Fig. S4 shows the UV-Vis absorption spectra of FG samples, suggesting the electronic configuration from polyene structures to polyaromatic ones with defluorination, where a broad band at 275 nm, a characteristic of the $\pi-\pi^*$ electron transition in the polyaromatic system, gains intensity while the band at 218 nm weakens.

6. Dispersion photographs of the FGi in PAO-40

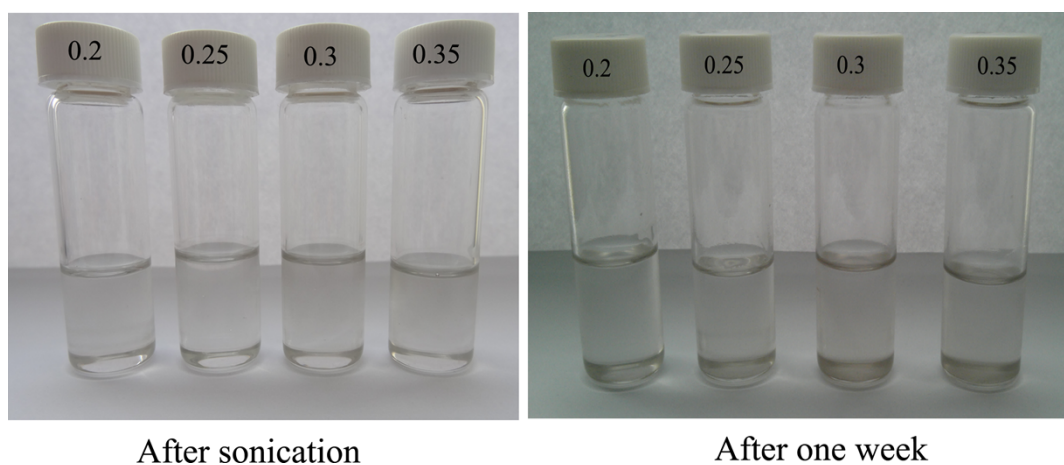


Fig. S5 shows the dispersion photographs of the raw material of FGi dispersed in PAO-40 immediately after the sonication (left) and one week after the sonication

(right). Considering that the optimum concentration of the three FG samples and effective comparison, different concentrations (0.2-0.35 mg/mL) of FGi dispersed in oil were prepared. It can be seen that the color of the products is light and the change is not apparent with the concentration gradient. While, it is worth noting that there is apparent precipitation observed at the bottom of the bottle after one week standing, suggesting poor dispersion stability of FGi in PAO-40.

7. Tribological performances of the oil dispersed with FGi.

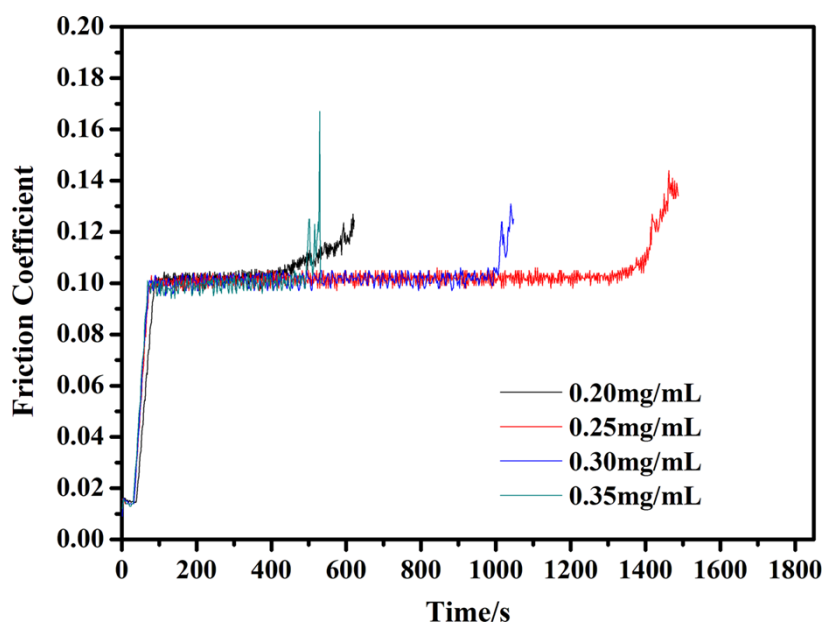


Fig. S6 is the evolution of friction coefficient with time at a given frequency of 20 Hz for PAO-40 with FGi at different concentrations. Under the same test condition, the addition of FGi makes the oil exhibit worse friction stability and durability, corresponding to the notable decrease of the time of stable friction state at different concentrations.

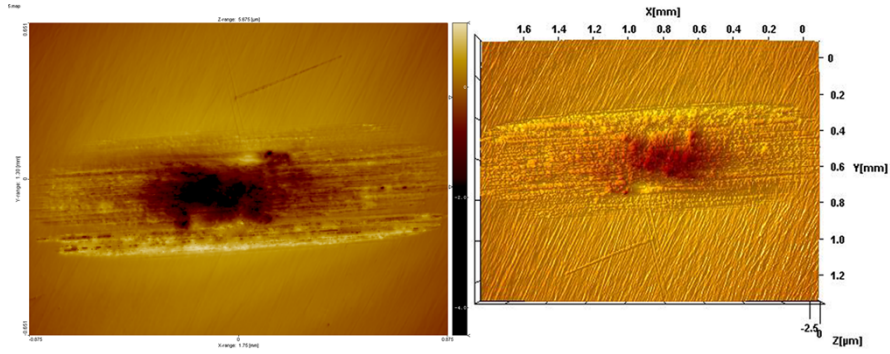


Fig. S7 is the height profile image and the corresponding 3D optical microscopic image of wear track on the lower disk lubricated by PAO-40 doped with FGi at 0.25 mg/mL. Due to the poor anti-wear performance as compared with FG, the wear scar of the base oil doped with 0.25 mg/mL FGi is rough with evident scratches originated from the unstable friction and vibration, as clearly shown in Fig. S4.